Supporting information

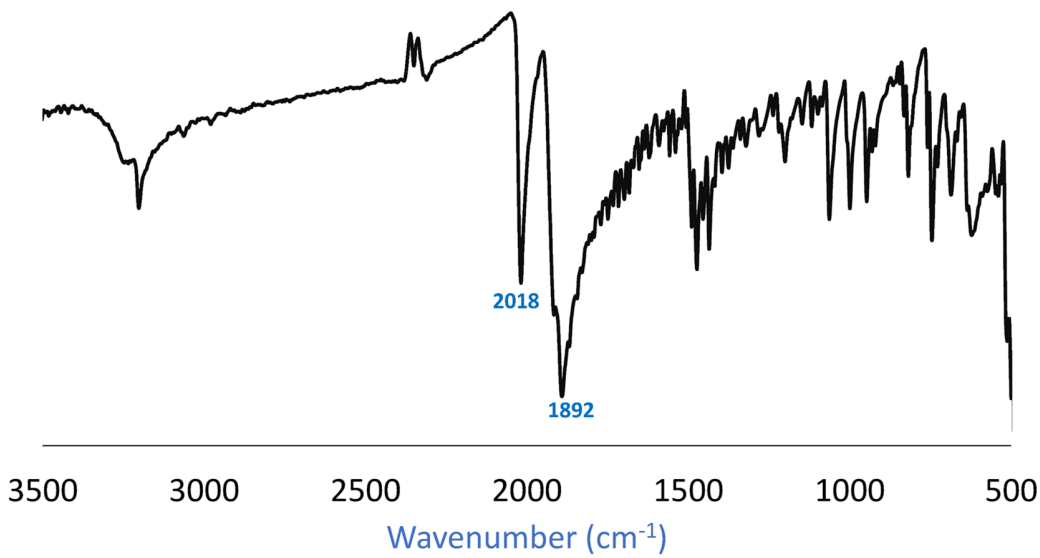

a)

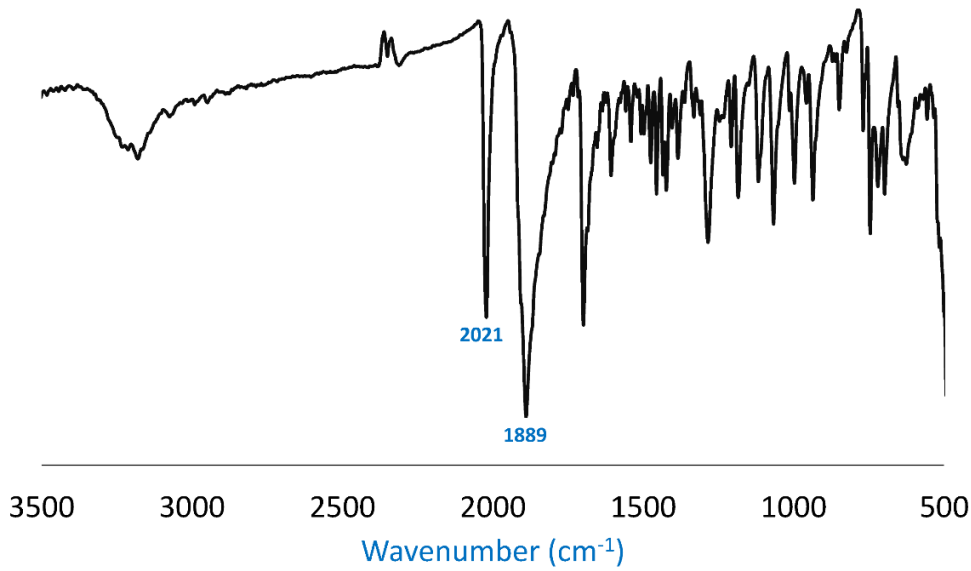

b)

Fig. S1 ATR-IR spectra of tricarbonyl rhenium(I) complexes a) **3**, and b) **4.**

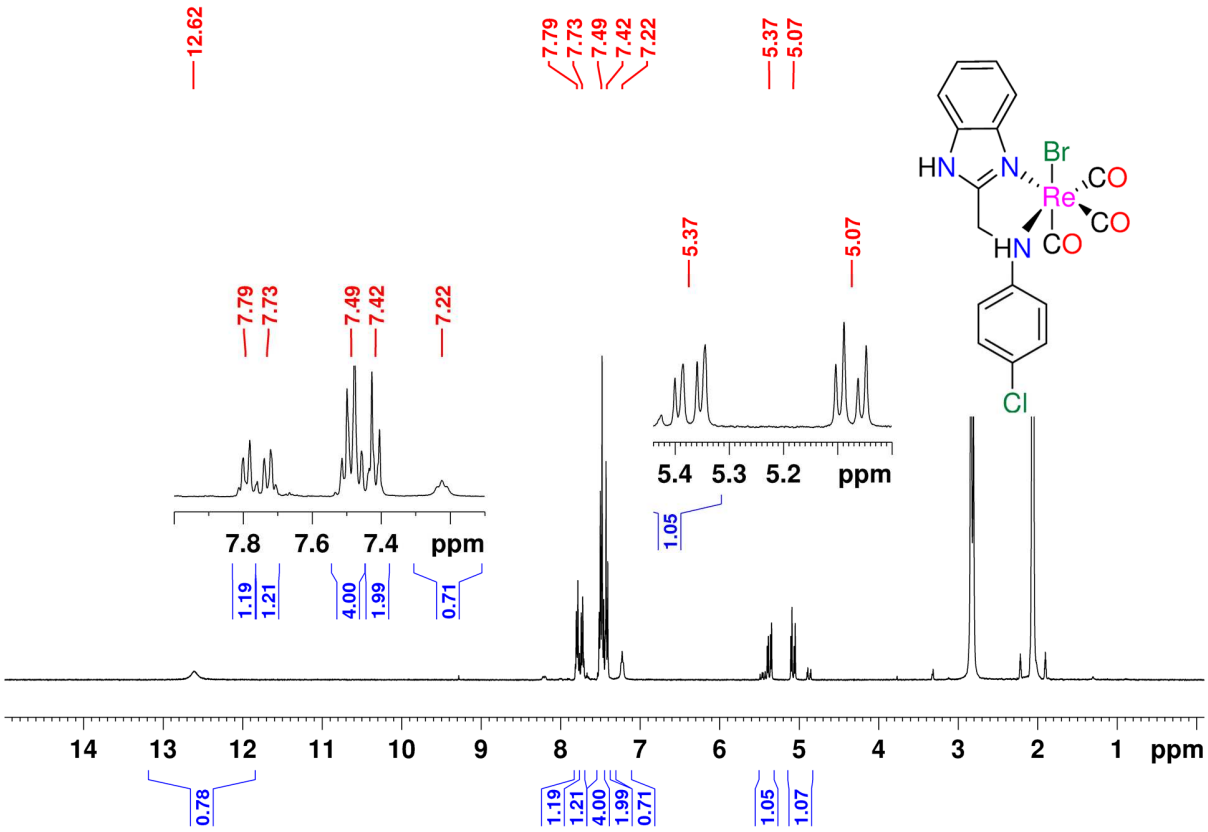

Fig. S2 ^{1}H NMR spectrum of **3** in acetone-d_6.

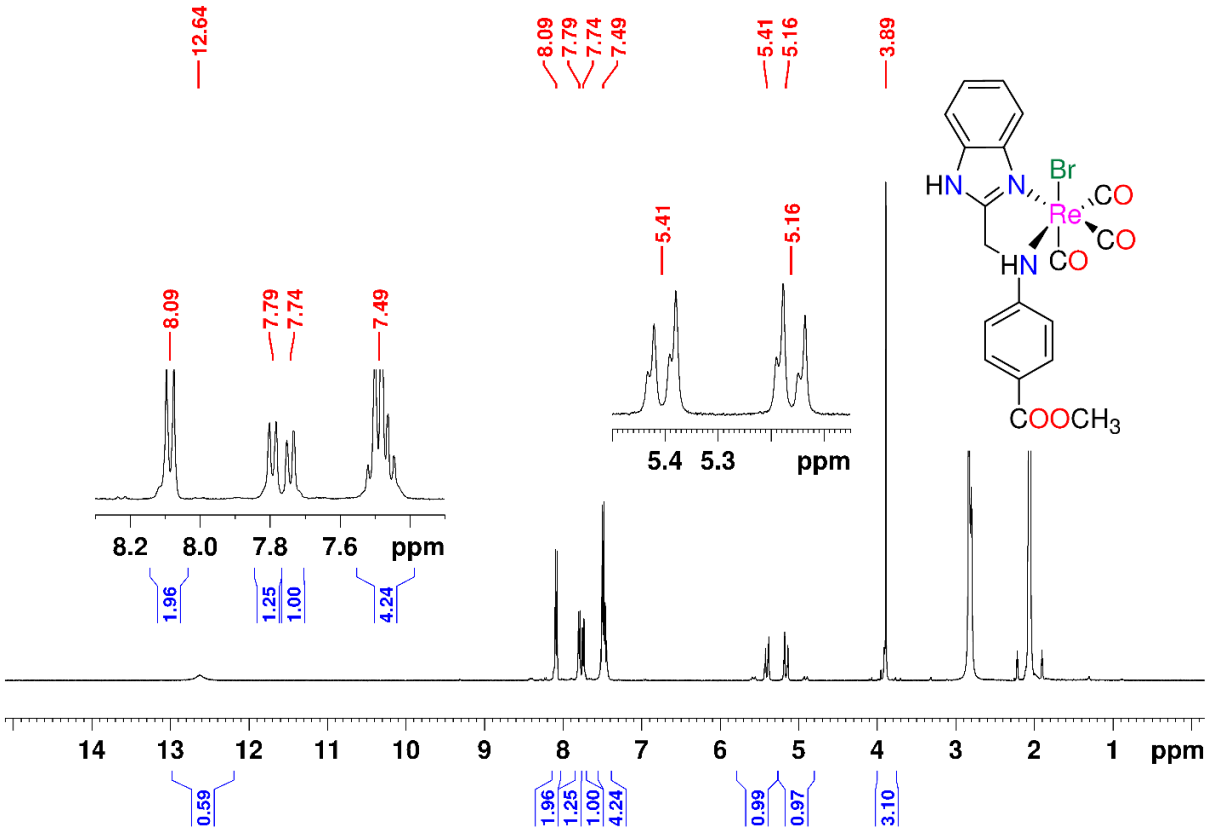

Fig. S3 ^{1}H NMR spectrum of **4** in acetone-d_6.

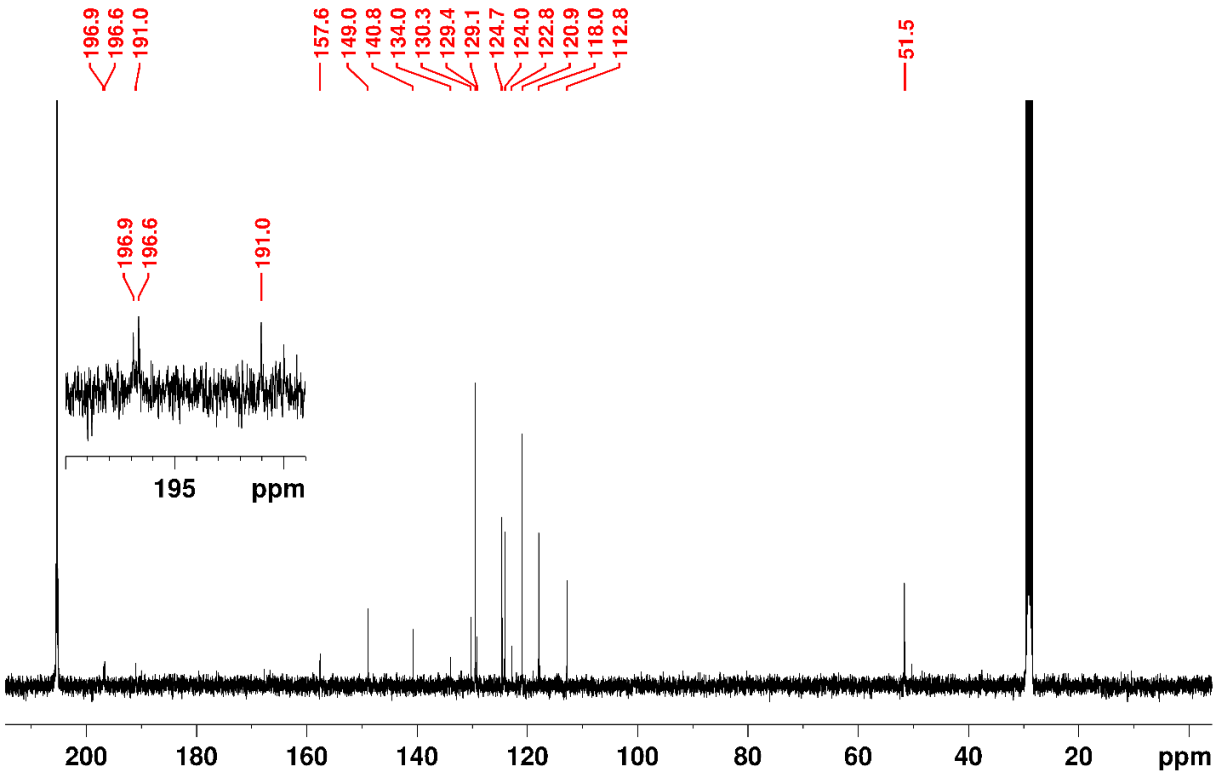

Fig. S4 ^{13}C NMR spectrum of **3** in acetone-d_6.

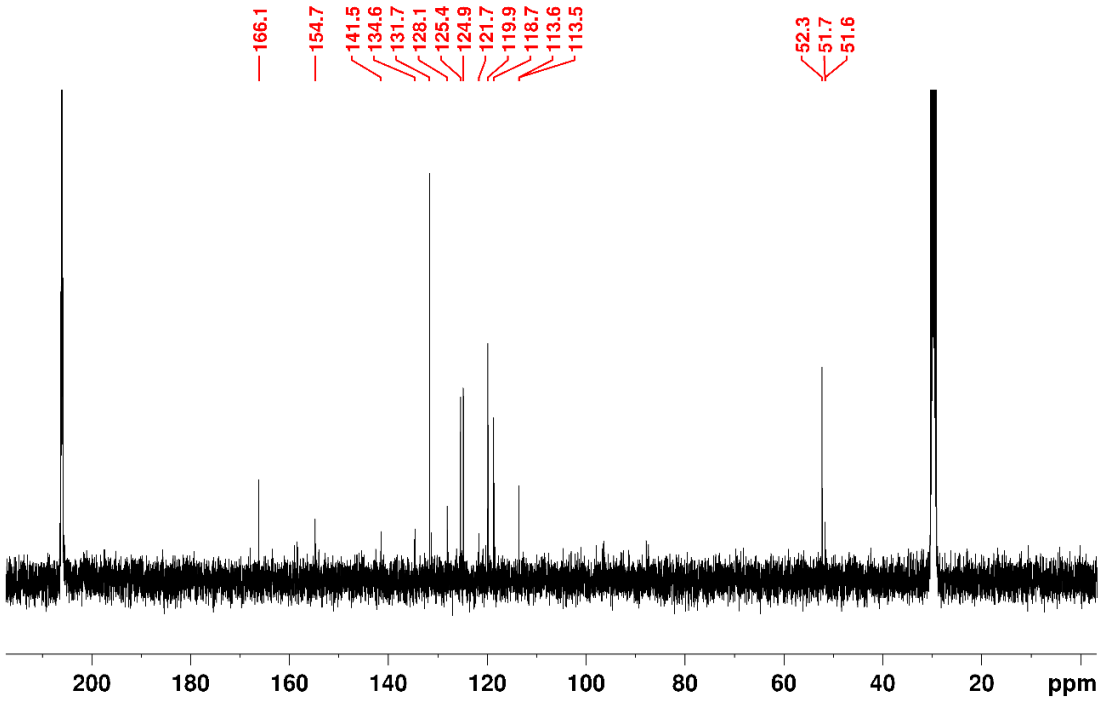

Fig. S5 ^{13}C NMR spectrum of **4** in acetone-d_6.

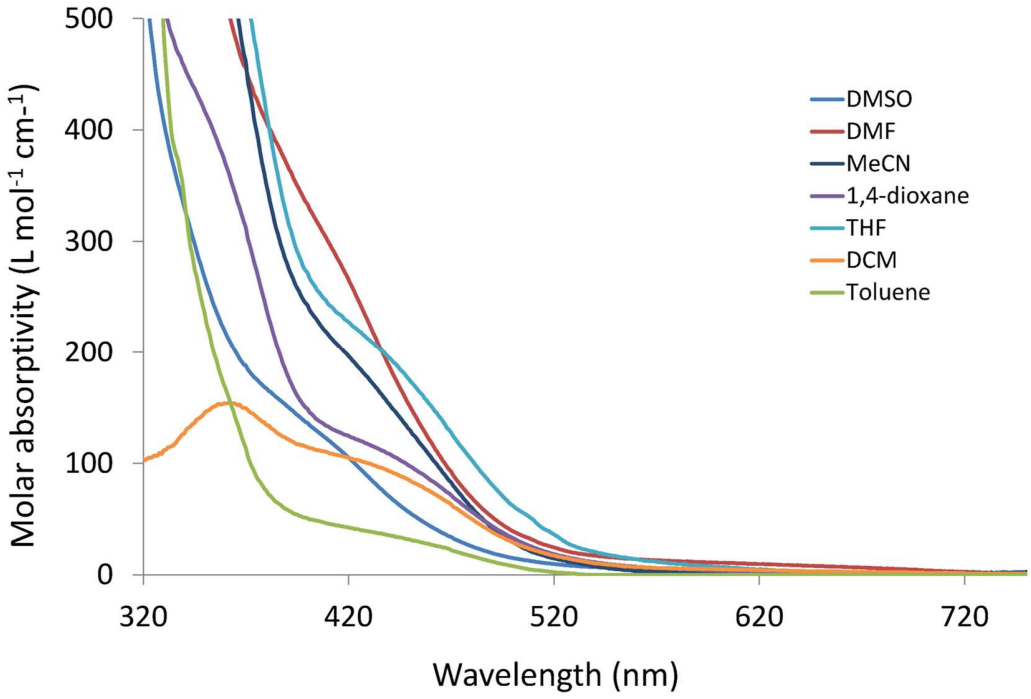

Fig. S6 Electronic absorption spectra of **3** in different solvents.

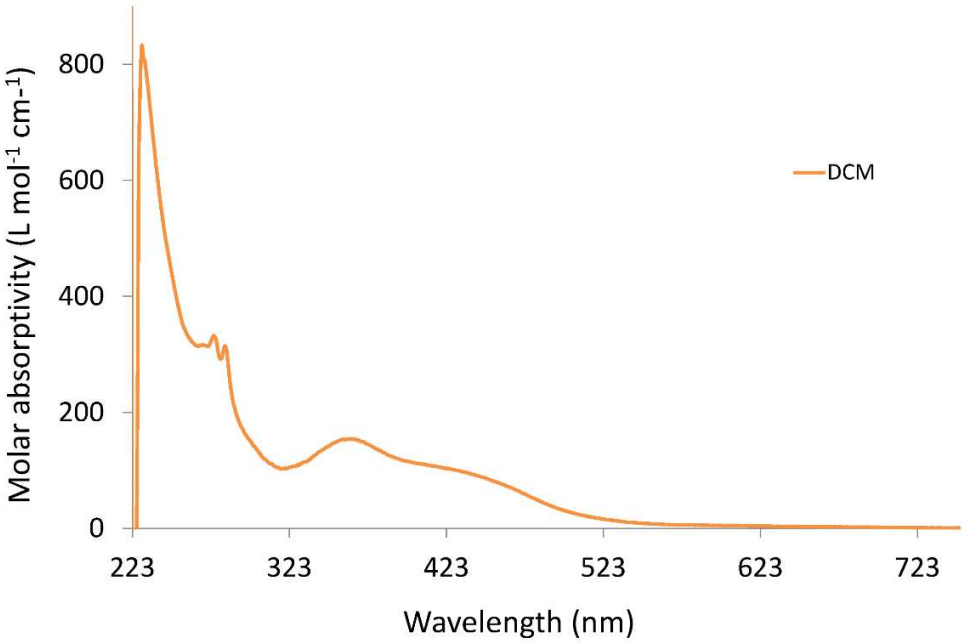

Fig. S7 Electronic absorption spectrum of **3** in dichloromethane.

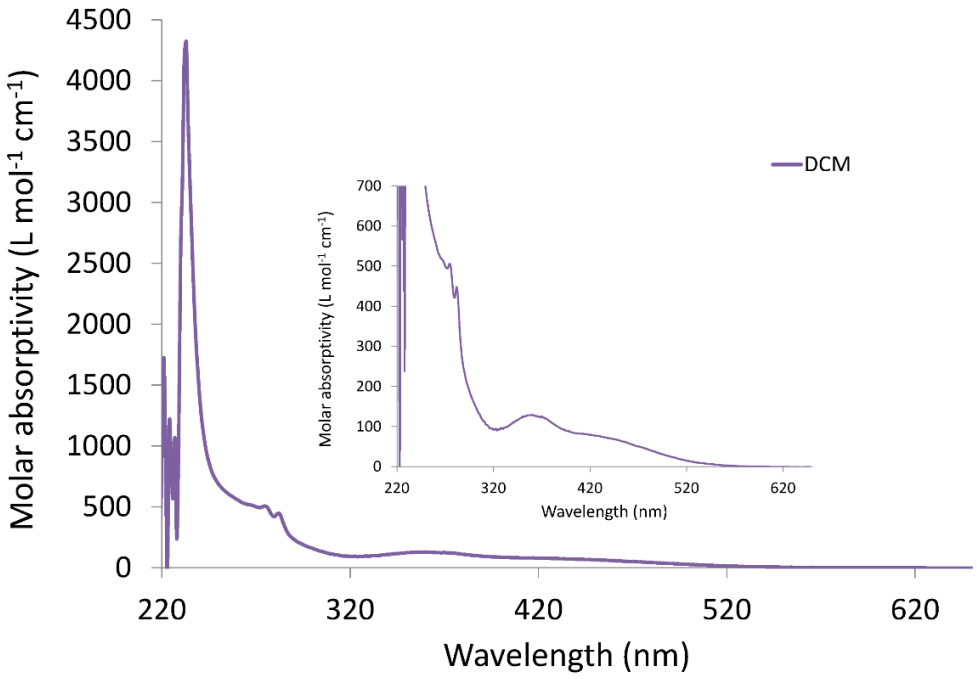

Fig. S8 Electronic absorption spectrum of **4** in dichloromethane.

Table S1 Atomic coordinates of the optimized structure of **3**.

Center Number	Atomic Number	Atomic Type	Coordinates (Angstroms)		
			X	Y	Z
1	8	0	-1.916633	-2.956455	-0.258332
2	8	0	2.398921	-2.955764	-1.242609
3	6	0	3.14213	0.944035	-0.2337
4	6	0	-2.885246	1.237185	-0.906194
5	6	0	-4.575999	0.634578	1.271055
6	7	0	2.26975	2.932181	0.365476
7	6	0	-4.278939	1.247178	-1.079717
8	6	0	5.510314	0.440355	-0.508827
9	7	0	-0.883956	0.921887	0.557984
10	6	0	-3.179413	0.639809	1.441487
11	6	0	5.827732	1.790013	-0.161472
12	6	0	-0.214787	2.24905	0.30152
13	7	0	1.742444	0.821265	-0.181066
14	6	0	-2.335394	0.943285	0.357129
15	6	0	4.828887	2.7269	0.151769
16	6	0	-5.106118	0.949471	0.013654
17	6	0	3.494493	2.286415	0.110713
18	6	0	4.177993	0.063153	-0.532874
19	6	0	-1.055391	-2.145287	-0.316963
20	6	0	1.25991	2.014029	0.175318
21	6	0	1.598185	-2.143447	-0.919213
22	1	0	-2.757233	0.389626	2.411847
23	1	0	-5.230396	0.391014	2.101384
24	1	0	-4.708941	1.4651	-2.051777
25	1	0	-2.245544	1.425025	-1.763627
26	1	0	6.303624	-0.263645	-0.742939
27	1	0	6.87121	2.09302	-0.139089
28	1	0	5.087429	3.747985	0.41624
29	1	0	2.149807	3.89453	0.652235
30	1	0	-0.675896	0.628459	1.528673
31	1	0	-0.610964	2.658187	-0.634263
32	1	0	-0.444997	2.965564	1.102755
33	75	0	0.335945	-0.811456	-0.376176
34	35	0	0.818145	-1.16627	2.291948
35	6	0	-0.070465	-0.372158	-2.176188
36	8	0	-0.337406	-0.06676	-3.300859
37	17	0	-6.909007	0.962405	-0.211399
Rotational constants (GHz)			0.2471111	0.0889260	0.0829737

Table S2 Atomic coordinates of the optimized structure of **3**.

Center Number	Atomic Number	Atomic Type	Coordinates (Angstroms)		
			X	Y	Z
1	8	0	-1.423883	-3.023069	-0.465851
2	8	0	2.826853	-2.70517	-1.665058
3	6	0	3.473221	1.068926	-0.228576
4	6	0	-2.580491	1.240744	-0.557496
5	6	0	-4.124321	0.114709	1.511332
6	7	0	2.5628	2.928711	0.65735
7	6	0	-3.975449	1.182707	-0.677143
8	6	0	5.840822	0.701534	-0.67239
9	7	0	-0.502	0.78082	0.753173
10	6	0	-2.729682	0.18005	1.639287
11	6	0	6.127456	2.009679	-0.172922
12	6	0	0.105173	2.154958	0.631775
13	7	0	2.08343	0.881518	-0.125091
14	6	0	-1.957094	0.746581	0.606292
15	6	0	5.113132	2.85855	0.30051
16	6	0	-4.7566	0.623801	0.357902
17	6	0	3.794776	2.371814	0.265228
18	6	0	4.523101	0.275363	-0.682886
19	6	0	-0.600597	-2.171541	-0.470938
20	6	0	1.577994	1.999256	0.401791
21	6	0	2.013293	-1.975145	-1.205472
22	1	0	-2.243961	-0.221091	2.525589
23	1	0	-4.734841	-0.324685	2.294385
24	1	0	-4.465388	1.552991	-1.570808
25	1	0	-1.990754	1.635099	-1.379955
26	1	0	6.64576	0.065336	-1.028874
27	1	0	7.159447	2.350246	-0.15941
28	1	0	5.348589	3.848587	0.679745
29	1	0	2.423815	3.841543	1.069841
30	1	0	-0.236504	0.380009	1.669839
31	1	0	-0.355557	2.663925	-0.221341
32	1	0	-0.103313	2.754361	1.529309
33	6	0	-6.240272	0.542841	0.271395
34	8	0	-6.981538	0.068128	1.152743
35	8	0	-6.730461	1.062492	-0.912194
36	6	0	-8.191	1.012803	-1.103195
37	1	0	-8.694228	1.577187	-0.311876
38	1	0	-8.362179	1.465842	-2.080577
39	1	0	-8.537247	-0.025167	-1.083531
40	75	0	0.731619	-0.777466	-0.443019
41	35	0	1.373898	-1.413715	2.138346
42	6	0	0.206952	-0.150826	-2.15592
43	8	0	-0.133918	0.268571	-3.22183

Rotational constants (GHz)	0.2374804	0.0690647	0.0656906

Table S3 Selected calculated bond lengths, and bond angles of complexes **3** and **4** calculated using B3LYP/LANL2DZ method.

	3	**4**
Re–C19	1.92832	1.92848
Re–C21	1.91372	1.91271
Re–C35 (Re–C42)	1.89689	1.89789
Re–Br	2.73446	2.73510
Re–N9	2.31631	2.31969
Re–N13	2.16381	2.16349
C19–O1	1.18455	1.18445
C21–O2	1.18559	1.18576
C35–O36 (C42–O43)	1.19558	1.19509
C19–Re–C21	90.18172	90.25669
C19–Re–C35 (C19–Re–C42)	91.99098	91.98524
C19–Re–Br	90.43087	90.44260
C19–Re–N9	97.19441	97.22122
C19–Re–N13	171.17513	171.14605
C21–Re–C35 (C21–Re–C42)	91.90470	91.84634
C21–Re–Br	94.02846	94.19794
C21–Re–N9	169.31287	169.28069
C21–Re–N13	97.01016	96.89459
C35–Re–Br (C42–Re–Br)	173.58420	173.47596
C35–Re–N9 (C42–Re–N9)	95.54113	78.13928
C35–Re–N13 (C42–Re–N13)	92.87072	92.99090
Br–Re–N9	78.25587	78.13928
Br–Re–N13	83.99028	83.85523
N9–Re–N13	75.00801	75.01254

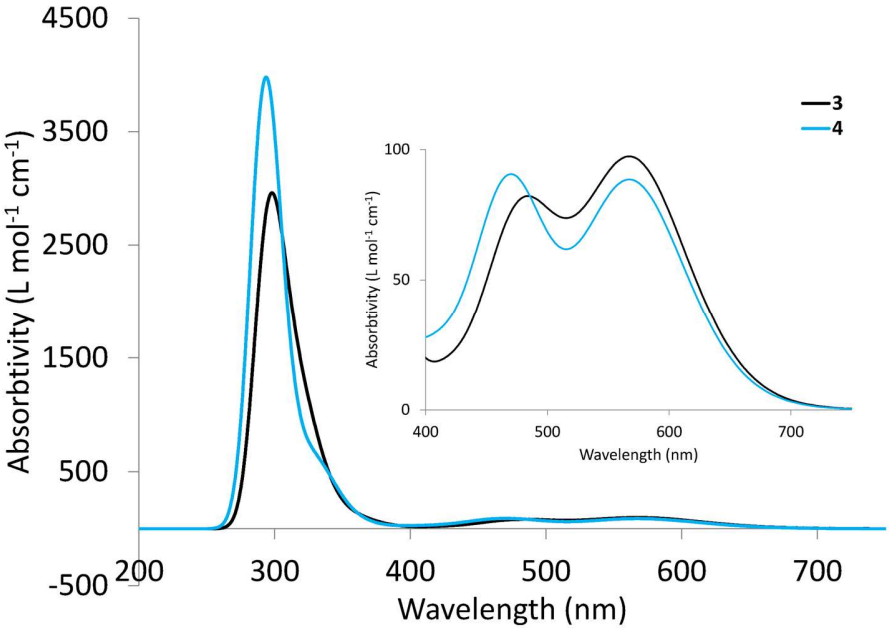

Fig. S9 Calculated electronic absorption spectra of **3** and **4** using B3LYP/LANL2DZ method in combination with SMD solvation model.

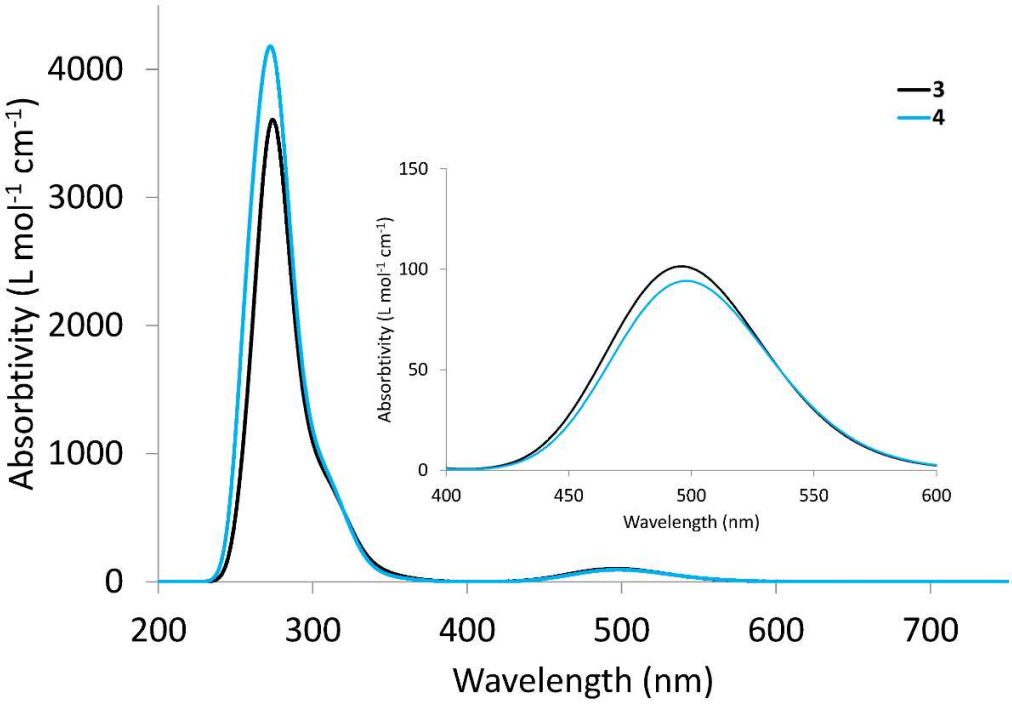

Fig. S10 Calculated electronic absorption spectra of **3** and **4** using CAM-B3LYP/LANL2DZ method in combination with SMD solvation model.

Table S4 Computed excitation energies (eV), electronic transition configurations and oscillator strengths (*f*) of rhenium(I) compounds (selected, *f* > 0.001) (Selected)			
Energy (cm^{-1})	Wavelength (nm)	*f*	Major contributions
• B3LYP/LANL2DZ method			
✓ **3**			
17569	569	0.0012	HOMO−2(β)→LUMO(β) (40%)
21181	472	0.0011	HOMO(β)→LUMO(β) (58%)
22305	448	0.0001	HOMO−1(β)→LUMO(β) (83%)
22679	440	0.0001	HOMO−4(β)→LUMO(β) (63%)
24672	405	0.0003	HOMO−3(β) →LUMO(β) (70%)
34310	291	0.0083	HOMO(α)→L+1(α) (36%)
✓ **4**			
17518	570	0.0013	HOMO−2(β) →LUMO(β) (30%), HOMO(β)→LUMO(β) (45%)
20766	481	0.001	HOMO−2(β)→LUMO(β) (22%), HOMO(β)→LUMO(β) (51%)
21781	459	0.0001	HOMO−1(β)→LUMO(β) (85%)
29714	336	0.0017	HOMO(α)→LUMO(α) (22%)
31167	320	0.0074	HOMO(α)→LUMO(α) (26%), HOMO(α)→LUMO+1(α) (23%)
33635	297	0.0109	HOMO−2(α)→LUMO+1(α) (20%)
• CAM-B3LYP/LANL2DZ method			
✓ **3**			
20099	497	0.0013	HOMO−2(β)→LUMO(β) (25%), HOMO(β)→LUMO(β) (21%)
26087	383	0	HOMO−4(β)→LUMO(β) (78%)
28876	346	0.0001	HOMO(α)→LUMO(α) (19%), HOMO(β)→LUMO+1(β) (22%)
29906	334	0.0001	HOMO−1(α)→LUMO(α) (22%), HOMO−1(β)→LUMO+1(β) (24%)
32157	310	0.0063	HOMO(α)→LUMO(α) (22%), HOMO(β)→LUMO+1(β) (24%)
34315	291	0.0021	HOMO−1(α)→LUMO+2(α) (22%)
34993	285	0.0051	HOMO−2(β)→LUMO(β) (21%)
38135	262	0.002	HOMO−6(β)→LUMO(β) (35%)
✓ **4**			
20179	495	0.0014	HOMO−3(β)→LUMO(β) (30%)
25437	393	0	HOMO−5(α)→LUMO(α) (22%), HOMO−5(β)→LUMO+1(β) (22%)

26222	381	0	HOMO−4(β)→LUMO(β) (78%)
32014	312	0.0057	HOMO(β)→LUMO+2(β) (21%)
34567	289	0.0054	HOMO−2(β)→LUMO(β) (26%)

Table S5 Selected frontiers molecular orbitals of **4** in the singlet state calculated at B3LYP/LANL2DZ level of theory.	
Orbital	Frontier molecular orbital
LUMO+2(β)	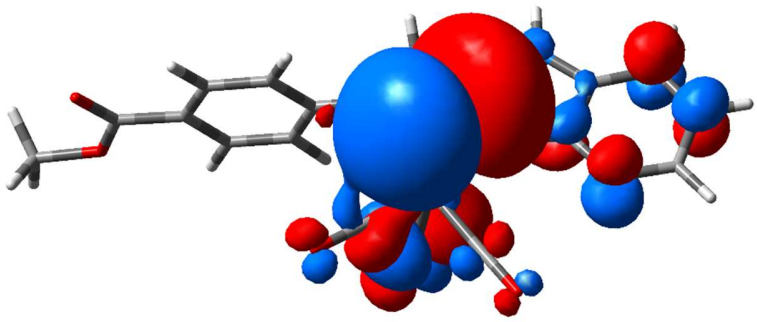
LUMO+1(β)	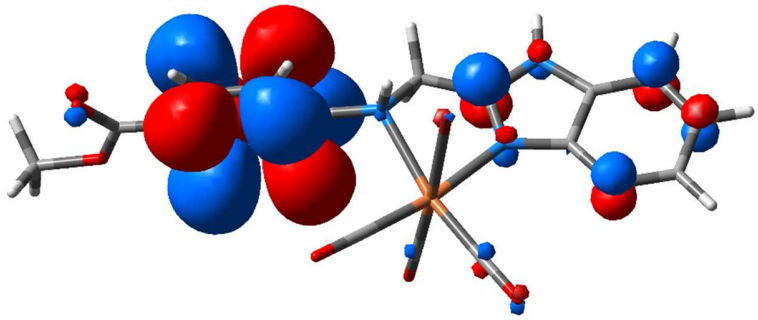
HOMO(β)	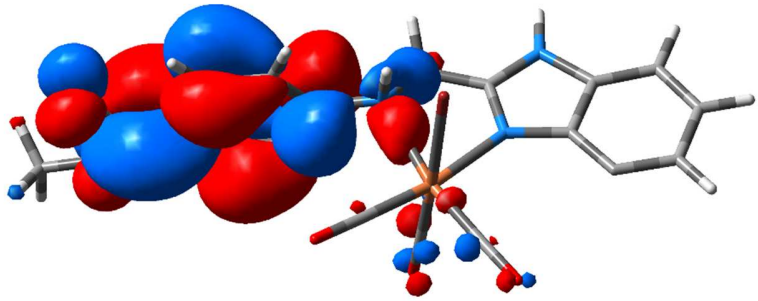
HOMO–1(β)	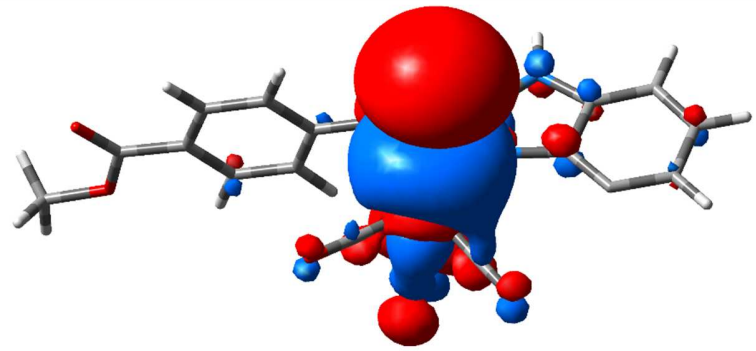

HOMO–2(β)	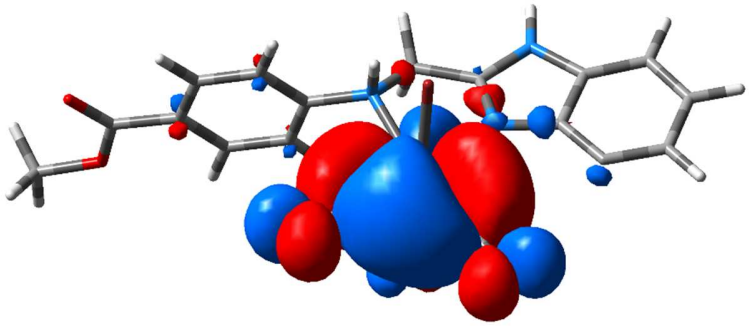
HOMO–3(β)	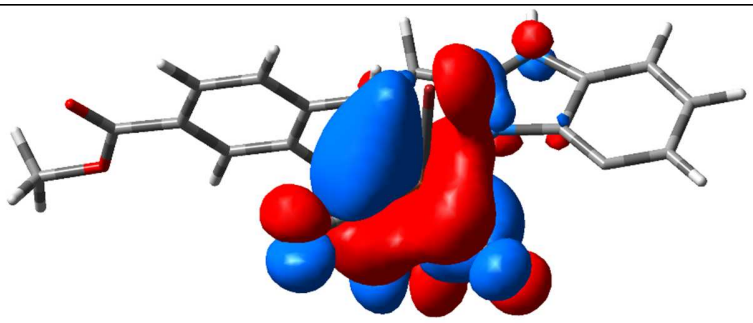
HOMO–6(β)	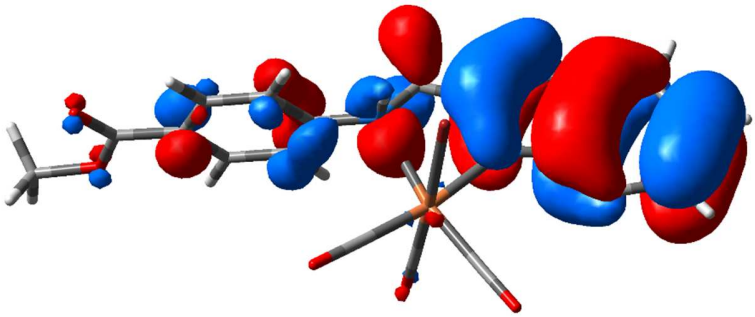
LUMO+1(α)	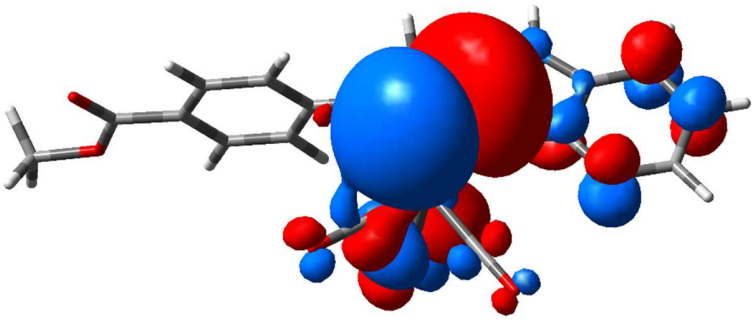

LUMO(α)	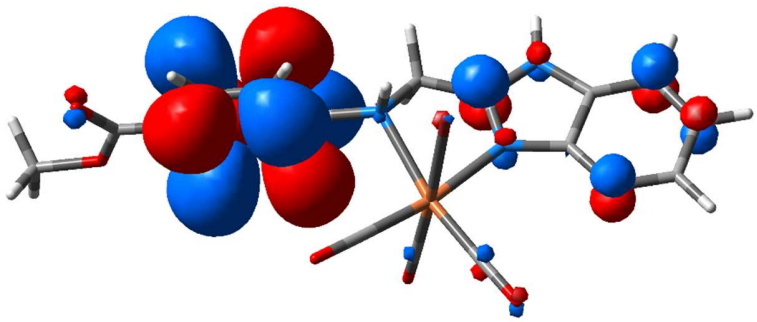
HOMO−2(α)	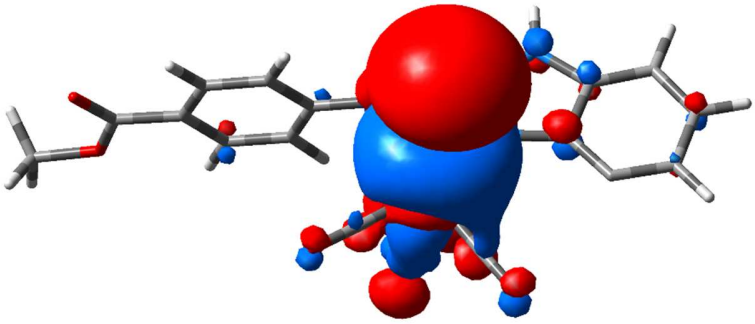
HOMO−5(α)	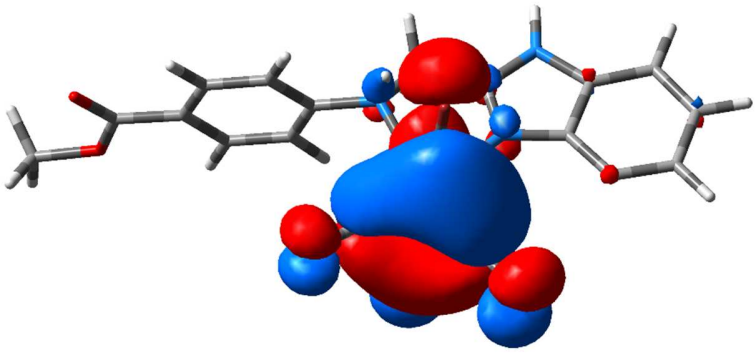

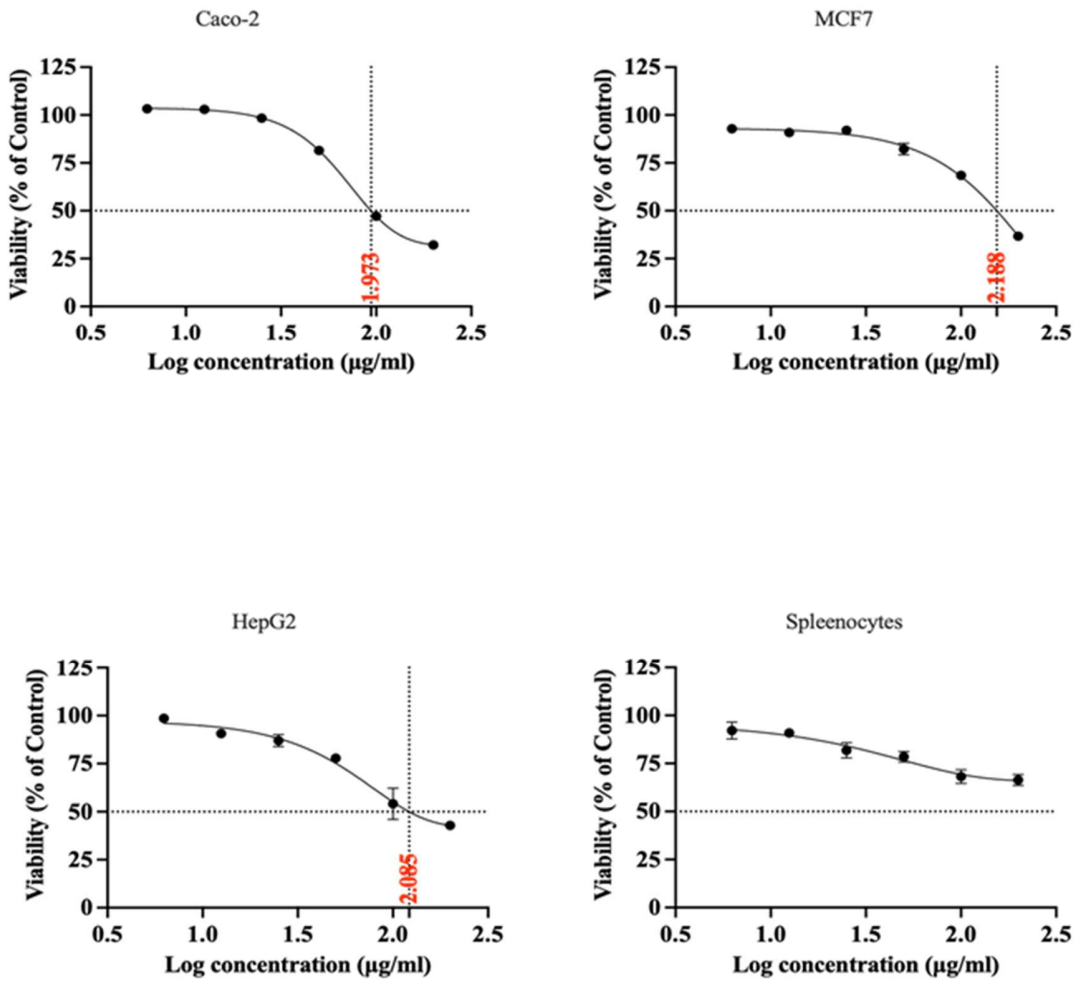

Fig. S10 The dose response curve of complex **3** on Caco-2, MCF7, HepG2 and splenocytes cell lines showing the IC_{50} at each cell line.

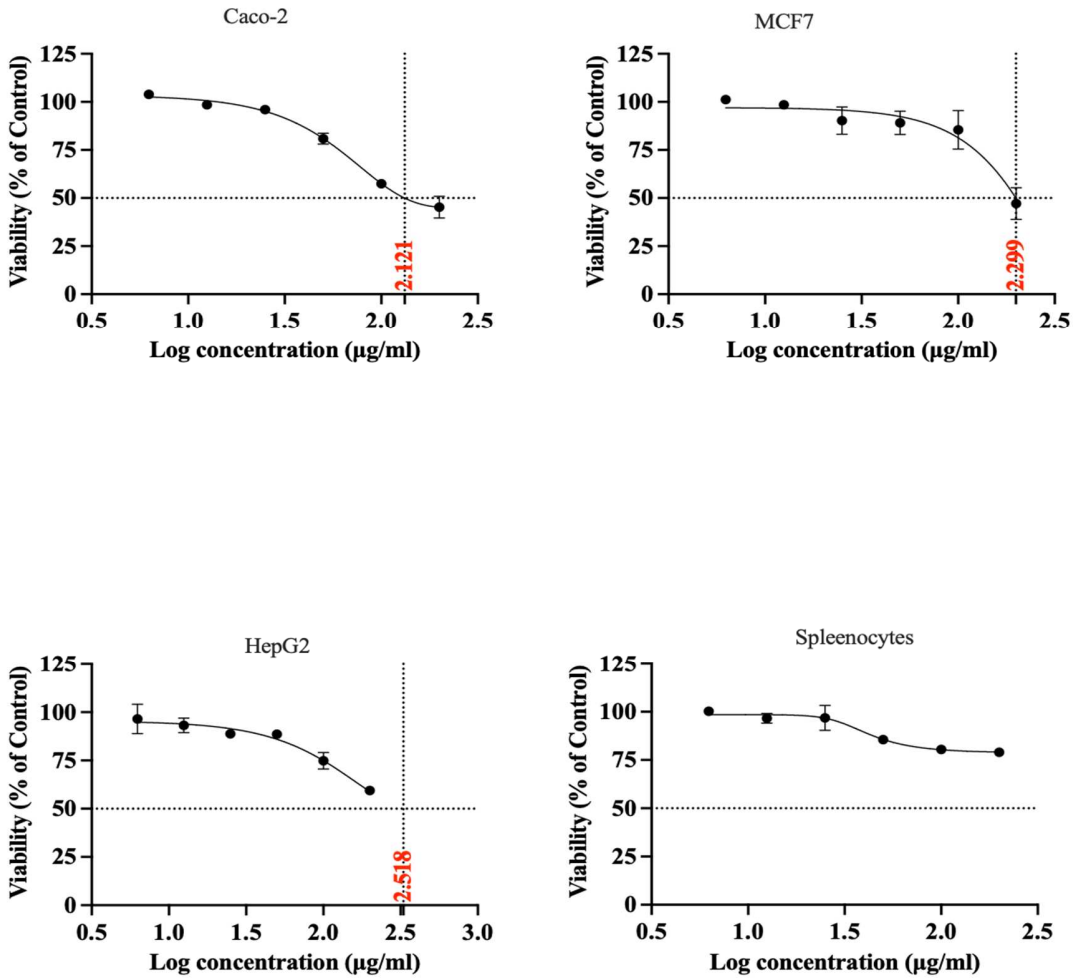

Fig. S11 The dose response curve of complex **4** on Caco-2, MCF7, HepG2 and splenocytes cell lines showing the IC_{50} at each cell line.

Table S6 The IC_{50} of compounds **3** and **4** each sample on different cell lines.

IC_{50} (μg/mL)	Caco-2	MCF7	HepG2	Splenocytes
3	93.74 ± 0.02	155.85 ± 1.07	124.6 ± 37.46	NA
4	149.73 ± 19.75	203.83 ± 9.87	289.3 ± 56.9	NA

• NA denotes Not available

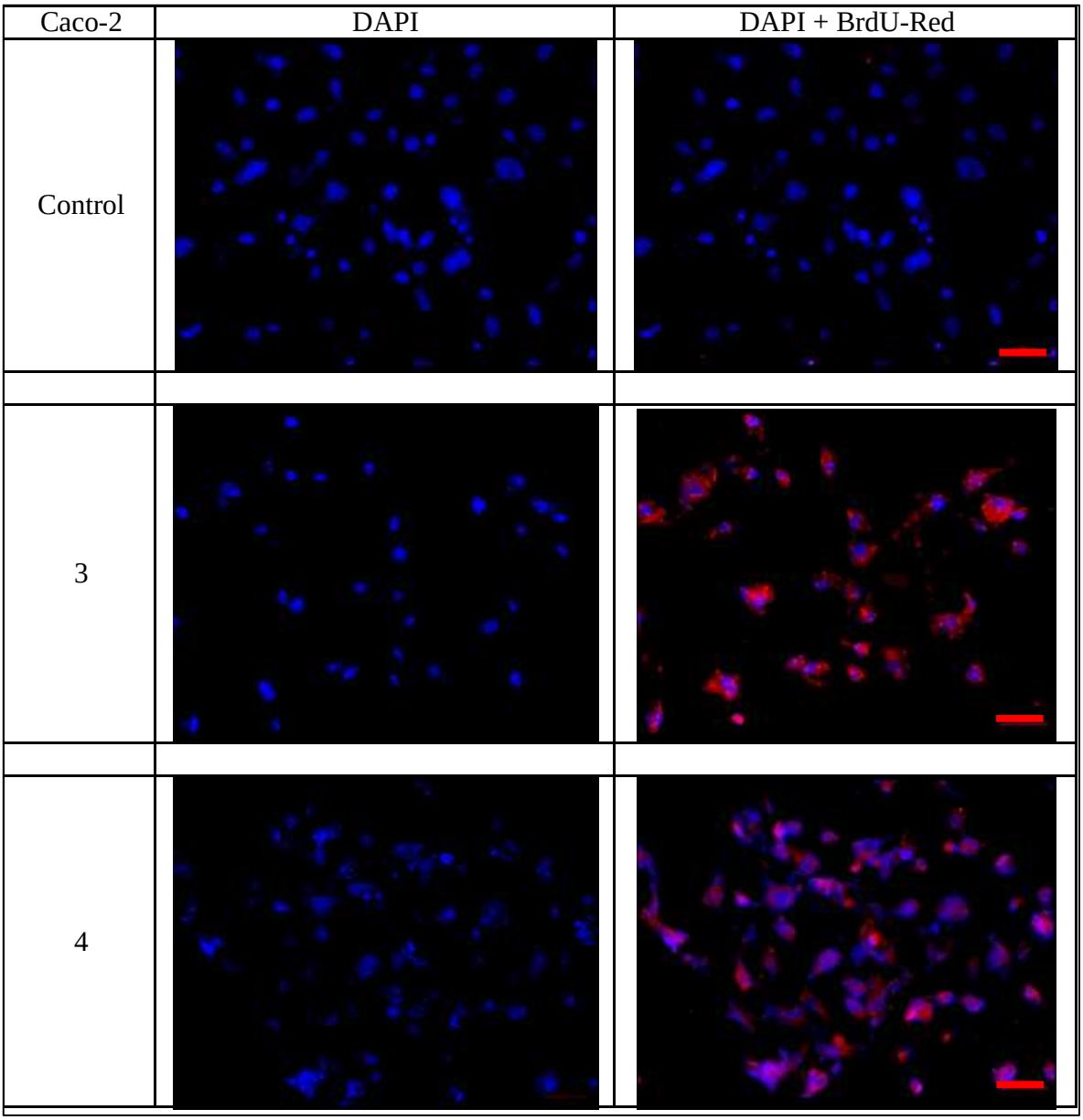

Fig. S12 The DNA fragmentation by TUNEL assay in Caco-2 cell line. The photos show high incorporation of BrdU-Red because of DNA fragmentation in comparison to the control. Magnification 20X. Scale bar 50 µm.

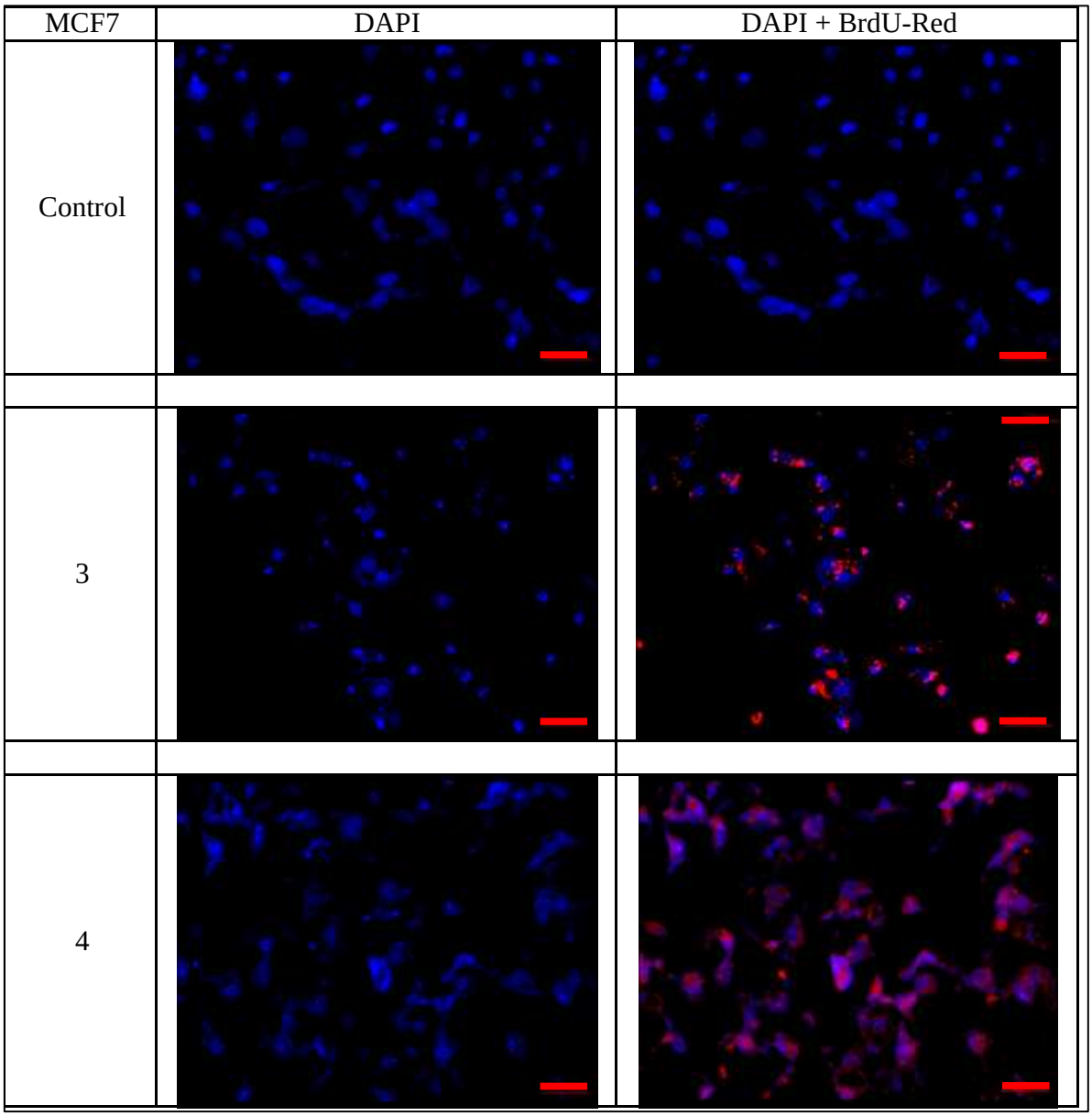

Fig. S13 The DNA fragmentation by TUNEL assay in MCF7 cell line. The photos show high incorporation of BrdU-Red in complex **4** more than complex **3** because of DNA fragmentation in comparison to the control. Magnification 20X. Scale bar 50 µm.

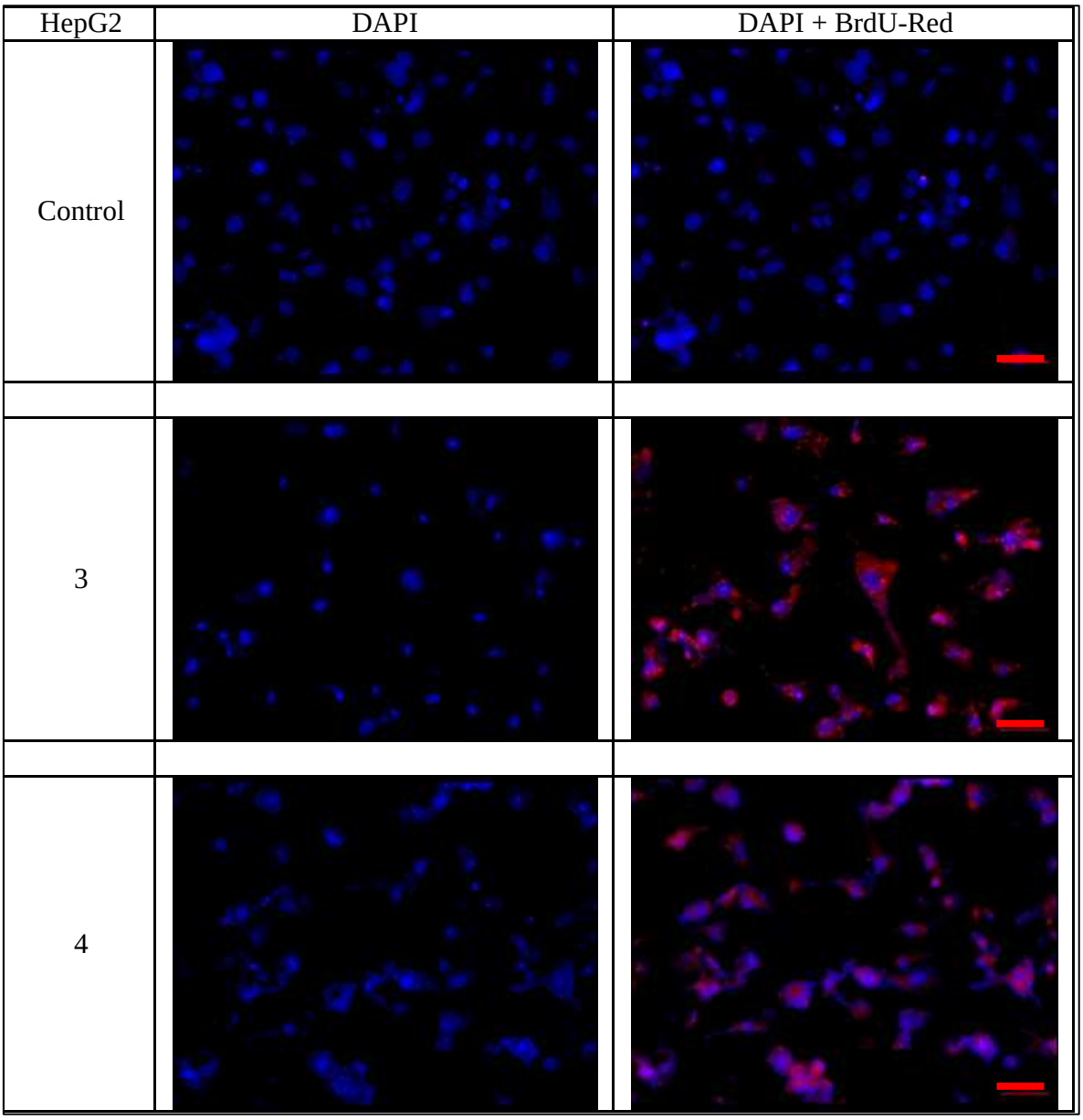

Fig. S14 The DNA fragmentation by TUNEL assay in HepG2 cell line. The photos show high incorporation of BrdU-Red because of DNA fragmentation in comparison to the control. Magnification 20X. Scale bar 50 µm.